Proceedings of IMECE 2002 ASME
November 17-22, 2002, New Orleans, LA

IMECE 2002 / DE-78102

AVOIDING FAILURES DURING ASSEMBLY OF A TRUNNION-HUB-GIRDER FOR BASCULE BRIDGES

Glen H. Besterfield
University of South Florida

Sanjeev Nichani
University of South Florida

Autar K. Kaw
University of South Florida

Thomas Eason
University of South Florida

Thomas Cherukara
Florida Dept. of Transportation

ABSTRACT

This paper is a study of avoiding failures during the assembly of a trunnion-hub-girder (THG) for bascule bridges. The currently used assembly procedure, AP#1, cools the trunnion for a shrink fit into the hub, followed by cooling of the trunnion-hub assembly to shrink fit it into the girder. During assembly, using AP#1, development of cracks on the hub was observed in one THG assembly. Yet, during another assembly, the trunnion got stuck in the hub before it could be fully inserted. A complete analytical, numerical, and experimental study was conducted to understand these failures, and the results were used to develop specifications and recommendations for assembly. The causes of failures include development of high stresses at low temperatures during assembly, while noting that fracture toughness of THG material decreases with temperature. Recommended specifications included following an alternative assembly procedure that doubled allowable crack length, and lower cooling temperatures to avoid trunnions sticking in the hub.

KEYWORDS

Bridge design, Bascule bridge, Stress analysis, Thermal stresses, Finite element analysis, Nonhomogenous properties, Strain measurement.

INTRODUCTION

In a bascule bridge, the fulcrum that is fit into its girder is made of a trunnion and a hub as shown in Figure 1. The trunnion, hub, and girder when fitted together are referred to as a trunnion-hub-girder (THG) assembly.

Current Assembly Procedure

The THG assembly is generally made by shrink fitting using interference fits (FN2 or FN3) between the trunnion and hub, and the hub and girder. The current procedure, henceforth called as AP#1, for assembling THG assemblies (in Florida) involves the following four steps (Figure 2)

1. The trunnion is shrunk by immersing in liquid nitrogen.
2. This shrunk trunnion is then inserted into the hub and allowed to warm-up to ambient temperature to develop an interference fit on the trunnion-hub interface.
3. The resulting trunnion-hub assembly is shrunk by immersing in liquid nitrogen.
4. This shrunk trunnion-hub assembly is then inserted into the girder and allowed to warm-up to ambient temperature to develop an interference fit on the hub-girder interface.

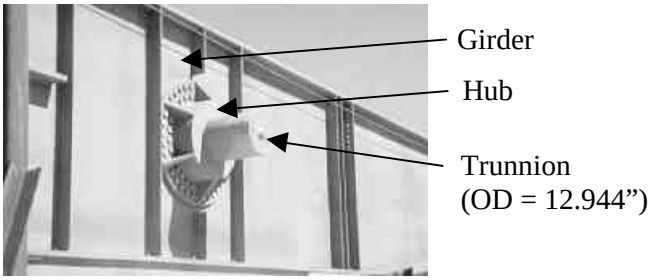

Figure 1. Trunnion-Hub-Girder (THG) assembly.

History

On May 3rd, 1995, during Step 3 of AP#1 for constructing the Christa McAuliffe Bridge in Florida, a cracking sound was heard as soon as the trunnion-hub assembly was immersed in liquid nitrogen. On removing the trunnion-hub assembly out of liquid nitrogen, the hub was found to have cracked near its inner radius.

Yet, in another case during Step 2 of AP#1 for constructing the Venetian Causeway Bridge, the trunnion got stuck before it could be fully inserted into the hub. In this case, a quick withdrawal of the trunnion saved the assembly from being rendered useless.

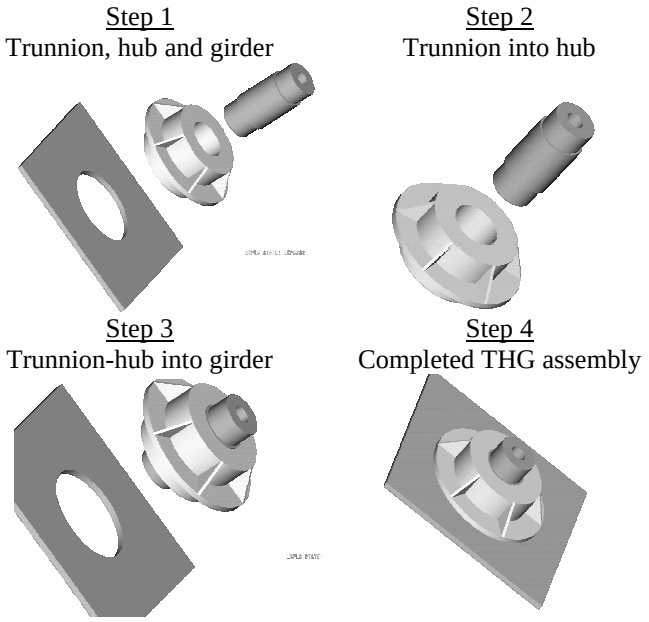

Figure 2. Steps of assembly procedure, AP#1.

Proposed Research

To avoid such failures in the future and develop specifications, the Florida Department of Transportation (FDOT) decided to investigate the cause of failure in the THG assemblies. Preliminary investigations done by independent consulting firms and manufacturers gave various reasons for the possible failure including high cooling rate, use of liquid nitrogen as a cooling medium, residual stresses in the cast hub, and the assembly procedure itself.

These preliminary investigations show that isolating and pinpointing the causes of failure intuitively is difficult for several reasons. First, it was observed that cracks were formed in some bridge assemblies but not in others. Second, the problem involves interplay of several issues that include complex geometries (gussets on the hub), transient stresses due to temperature coupled with stresses due to interference, and temperature-dependent material properties of the THG material (coefficient of thermal expansion, specific heat, thermal conductivity, yield strength and fracture toughness).

Hence, from August 1998 to Nov. 2001, with funding from the FDOT, the University of South Florida conducted an extensive and complete study of the problem. The study included – an analytical study based on steady-state stresses [1], a numerical study to incorporate transient stresses and complex geometry [2], and an experimental study [3] to verify the theoretical results. Readers interested in the complete extensive report [4] can visit the bascule bridge web-site [5].

NOMENCLATURE

a	crack length
a_c	critical crack length
c_1^i, c_2^i	unknown constants for cylinder i, i=1,2,3
C	fit coefficient
D	nominal diameter
E_j	Young's modulus of cylinder j, j=1, 2, 3
f_e	edge effect factor
K_I	stress intensity factor
K_{Ic}	critical stress intensity factor (fracture toughness)
L	limit
r_i^j	inner radius of cylinder j, j=1, 2, 3
r_o^j	outer radius of cylinder j, j=1, 2, 3
u_r^i	radial displacement in cylinder i, i=1,2,3
ν_j	Poisson's ratio of cylinder j, j=1, 2, 3
σ_e^i	Von Mises stress in cylinder i, i=1,2,3
σ_r^i	radial stress in cylinder i, i=1,2,3
σ_θ	hoop stress
σ_θ^i	hoop stress in cylinder i, i=1,2,3

ANALYTICAL STUDY

In this study, called "Bascule Bridge Design Tools" (BBDT), approximate steady-state stress equations were developed for calculating the critical hoop and Von Mises stresses to determine the failure of the assembly.

Interference Fits

Due to the shrink-fit, compressive radial stresses are developed at the trunnion-hub and hub-girder interfaces. Such compressive radial stresses transfer the design load (dead load, wind load, dynamic load, etc.) from the girder to the trunnion.

The diameteral interferences at the trunnion-hub and hub-girder assemblies are based on standard interference fits – FN2 or FN3 [6]. These standard interference fits dictate the limits of the dimensions of the THG parts as follows.

If a cylinder 'B' is fit into cylinder 'A', there is an upper and lower limit by which the nominal (outer or inner, respectively) diameter of each cylinder varies. This limit, L, in thousands of an inch, is given by

$$L = CD^{1/3}$$

where D (nominal diameter) is in inches and the coefficient C, based on the type of fit, is given in Table 1 [6].

For a typical nominal trunnion outer diameter and hub inner diameter of 12.944 in, using a FN2 fit, the four limits are calculated as follows.

$$L = (0)\,(12.944)^{1/3}\,(0.001) = 0.00000 \text{ in}$$
$$L = (0.907)\,(12.944)^{1/3}\,(0.001) = 0.00213 \text{ in}$$
$$L = (2.717)\,(12.944)^{1/3}\,(0.001) = 0.00638 \text{ in}$$
$$L = (3.288)\,(12.944)^{1/3}\,(0.001) = 0.00772 \text{ in}$$

Hence, the outer diameter dimensions of the trunnion would be $12.944^{+0.00772}_{+0.00638}$ in., and the inner diameter of the hub would be $12.944^{+0.00213}_{+0.00000}$ in. These two pairs of extreme dimensions of the trunnion and hub diameters produce values of diametrical interference ranging from 0.00425 in. to 0.00772 in. The dimensions of a typical THG assembly are given in Table 2. These dimensions are taken from the full-scale model used in conducting the experiments and is used to illustrate results from all the three parts of the study.

Table 1. Coefficient (C) to calculate limits (L).

Cylinder	Limit	Class of fit	
		FN2	FN3
A	Lower	0.000	0.000
	Upper	0.907	0.907
B	Lower	2.717	3.739
	Upper	3.288	4.310

Table 2. Dimensions of the full-scale trunnion, hub, and girder based on FN2 fit.

Component	Inner diameter (inches)	Outer diameter (inches)
Trunnion	2.375	$12.944^{+0.00772}_{+0.00638}$
Hub	$12.944^{+0.00213}_{+0.00000}$	$17.760^{+0.00858}_{+0.00709}$
Girder	$17.760^{+0.00237}_{+0.00000}$	60.000[1]

For calculating the approximate steady-state stresses in the THG assembly, the trunnion, hub, and girder are approximated by axisymmetric circular cylinders (Figure 3) with the material and geometrical properties given in Table 3.

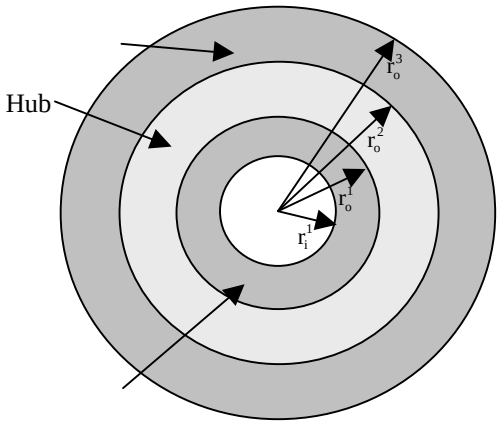

Figure 3. Axisymmetric cylinders representing the Trunnion-Hub-Girder assembly.

The nominal radii of the three cylinders have the following relationships:

$$r_i^2 = r_o^1 \quad (1a)$$

$$r_i^3 = r_o^2 \quad (1b)$$

The inner radius of the trunnion (Cylinder 1) can be zero if the cylinder is solid.

Table 3. Geometrical and elastic parameters of three cylinders.

Parameter	Trunnion Cylinder 1	Hub Cylinder 2	Girder Cylinder 3
Nominal inner radius	r_i^1	r_i^2	r_i^3
Nominal outer radius	r_o^1	r_o^2	r_o^3
Young's modulus	E_1	E_2	E_3
Poisson's ratio	ν_1	ν_2	ν_3

Steady-state Stresses

The stresses (radial, hoop, and Von Mises) and the radial displacements in each cylinder (assuming plane stress) can then be found as follows.

For each cylinder 'i', the radial displacement (u_r) is of the form [7]

$$u_r^i = c_1^i r + \frac{c_2^i}{r}, i = 1,2,3 \quad (2)$$

from which the radial stress is given as

$$\sigma_r^i = \frac{E_i}{1-\nu_i^2}\left[c_1^i(1+\nu_i) - c_2^i\left(\frac{1-\nu_i}{r^2}\right)\right], i = 1,2,3 \quad (3)$$

The boundary conditions of zero radial stress on the inside and outside radii of the THG assembly, continuity of radial stresses and the shrinking allowance, at the two interfaces, solves for the six unknown constants (c_1^i , c_2^i, i = 1,2,3).

The hoop (σ_θ), and Von Mises (σ_e) stresses, respectively, for each of the three members is given by

$$\sigma_\theta^i = \frac{E_i}{1-\nu_i^2}\left[c_1^i(1+\nu_i) + c_2^i\frac{(1-\nu_i)}{r^2}\right], i = 1,2,3 \quad (4a)$$

$$\sigma_e^i = \left[(\sigma_r^i)^2 - (\sigma_r^i)(\sigma_\theta^i) + (\sigma_\theta^i)^2\right]^{1/2}, i = 1,2,3 \quad (4b)$$

Based on the dimensions shown in Table 2, a summary of the approximate critical steady-state stresses in the THG assembly is shown in Table 4.

Table 4. Approximate critical steady-state stresses.

Maximum stresses (ksi)	Trunnion	Hub	Girder
Compressive radial	14.165	10.342	10.342
Tensile hoop	0.000	5.118	12.329
Compressive hoop	29.318	3.853	0.000
Von-Mises	29.318	15.350	19.659

All of these stresses are well below the yield strength of 36 ksi of the THG cast steel and hence imply that steady-state stresses are not a cause of failure. This prompted a finite

[1] The girder was approximated by a flat plate (60" ×60" × 0.75") with a hole of diameter 17.76".

element study of the problem to find if the transient stresses exceeded allowable stresses. Before introducing the finite element analysis study, several technical issues are addressed.

TECHNICAL BACKGROUND

Alternate Assembly Procedure

An alternate assembly procedure, henceforth called as AP#2, for assembling THG assemblies (in Florida) involves four steps that are similar to AP#1, however, performed in a different order (Figure 4).

1. The hub is shrunk by cooling in liquid nitrogen.
2. This shrunk hub is then inserted into the girder and allowed to warm-up to ambient temperature to develop an interference fit on the hub-girder interface.
3. The trunnion is shrunk by cooling in liquid nitrogen.
4. This shrunk trunnion is then inserted into the hub-girder assembly and allowed to warm-up to ambient temperature to develop an interference fit on the trunnion-hub interface.

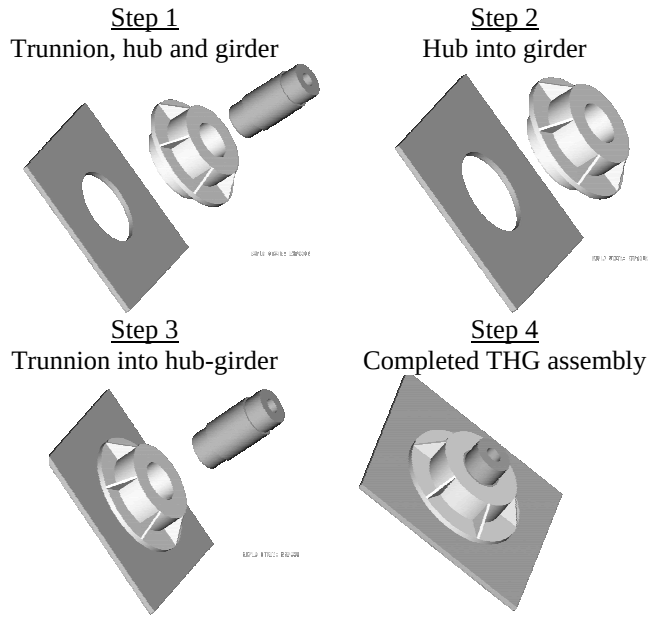

Figure 4. Steps of assembly procedure, AP#2.

Critical Crack Length and Fracture Toughness

Small cracks present in the assembly can propagate catastrophically once they attain a critical crack length, a_c. The critical crack length is calculated as follows. For an edge radial crack in a hollow cylinder that is small in comparison to the radial thickness of the cylinder (see Figure 5), the stress intensity factor at the crack tip is given by

$$K_I = f_e \, \sigma_\theta \sqrt{\pi a} \qquad (5)$$

where a, f_e, K_I, and σ_θ are the crack length, edge effect factor, stress intensity factor, and hoop stress, respectively. Note that f_e equals 1.125 for an edge crack (worst case scenario).

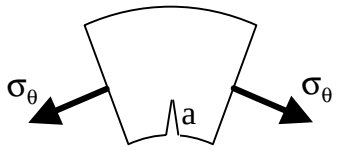

Figure 5. Critical crack length.

If $K_I = K_{Ic}(T)$, where $K_{Ic}(T)$ is the temperature dependent critical stress intensity factor or fracture toughness of the material, then the critical crack length (that is, the maximum crack length allowable before a crack propagates catastrophically) is determined by the previous equation [8].

$$a_c = \frac{K_{Ic}^2(T)}{f_e^2 \pi \sigma_\theta^2} \qquad (6)$$

The critical stress intensity factor, K_{Ic}, in turn is a function of temperature. K_{Ic} decreases with a decrease in temperature as shown in Figure 6, whereas yield strength increases with a decrease in temperature.

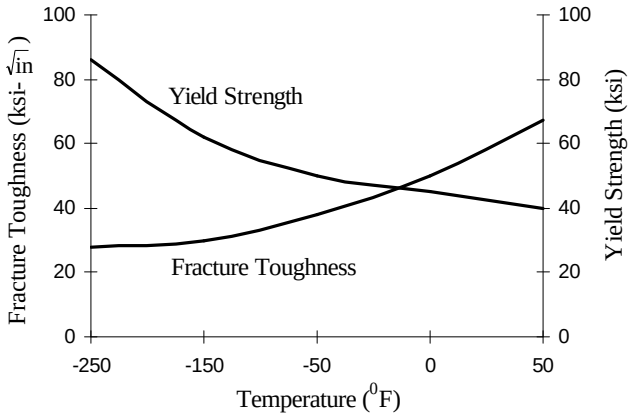

Figure 6. Fracture toughness and yield strength variation of steel as a function of temperature – reproduced by permission of ASM International [9].

Nonlinear Material Properties

The material properties of the THG assembly, the air, and the cooling medium are temperature dependent. Though nonlinear material properties in general are explored, particular emphasis is given to properties at low temperatures. For instance, in Figure 7, the variation of the coefficient of thermal expansion with temperature is presented. It is important to note from Figure 7 that less expansion (contraction) is realized at low temperatures.

The variation in the other material properties of steel relevant to this study, as the temperature increases from -321°F to 80°F, are described below:

- Young's modulus decreases almost linearly from approximately 32 to 30 Msi.
- Thermal conductivity of steel increases nonlinearly with decreasing slope from approximately 1.0 to 1.9 BTU/hr/in/^{0}F.

- Density of steel remains relatively constant at approximately 0.28 lb/in^3.
- Specific heat of steel increases nonlinearly with decreasing slope from approximately 0.025 to 0.11 BTU/lb/^{0}F.

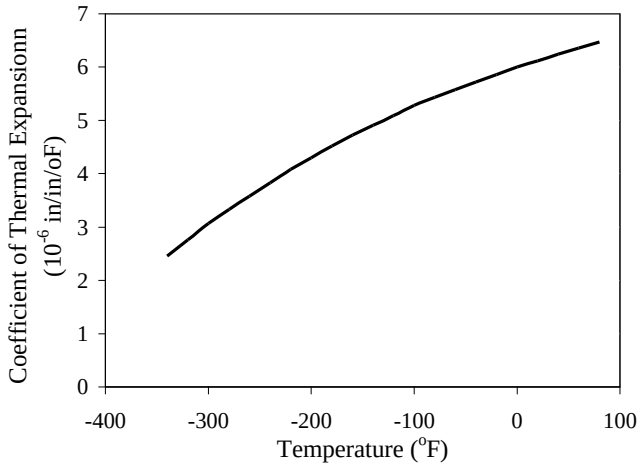

Figure 7. Coefficient of thermal expansion of steel as a function of temperature.

The convection heat transfer coefficient of air decreases nonlinearly with increasing slope from approximately 0.008 to 0.0012 BTU/hr/in^2/^{0}F as the temperature increases from -120^{o}F to 80^{o}F. The calculation of the convection heat transfer coefficient of air is based on the Nusselt, Prandtl, and Grashoff numbers which were calculated using the following properties: volumetric coefficient of thermal expansion of air, kinematic viscosity of air, specific heat of air, absolute viscosity of air, and mass density of air. The range for the convection coefficient is only -120^{o}F to 80^{o}F, because it is calculated based on the average of the wall temperature and the bulk or ambient temperature. The following other assumptions were also made in the calculation of the convection heat transfer coefficient of air:

- The value for the hydraulic diameter, D, for the trunnion is the outer diameter of the trunnion; for the hub, it is the hub outer diameter; and for the girder, it is the length of the girder.
- Turbulent flow is assumed.

Figure 8 shows a typical curve of heat flux from liquid nitrogen versus the change in temperature between the wall temperature and the saturation temperature (i.e., -321^{o}F) of liquid nitrogen [10]. Notice the region of nucleate, transition, and film boiling. The convection heat transfer coefficient of liquid nitrogen is simply the heat flux divided by the change in temperature. Based on Figure 8, the convection heat transfer coefficient of liquid nitrogen increases nonlinearly with decreasing slope from 0.069 to 0.597 BTU/hr/in^2/^{0}F, as the wall temperature increases from -321^{o}F to 80^{o}F. However, there is a spike resulting from large change in the heat flux with a relatively small change in the temperature during the transition boiling region from approximately -270^{0}F to -290^{0}F. Note that the convection heat transfer coefficient of liquid nitrogen is evaluated at the wall temperature.

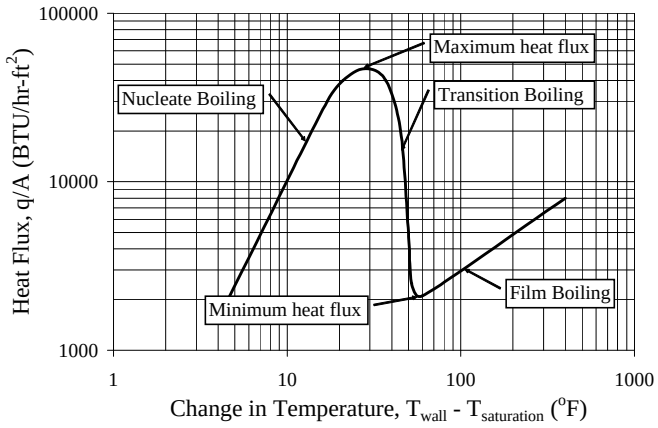

Figure 8. Heat flux as a function of the change in temperature between the wall and the saturation temperature of liquid nitrogen.

FINITE ELEMENT STUDY

The transient thermal-structural problem of assembling the trunnion, hub, and girder is performed via a parametric finite element code, called "Trunnion-Hub-Girder Testing Model" (THGTM), which uses a graphical user interface [2].

Input Parameters

The input parameters to the THGTM code consist of the following geometric parameters, non-homogeneous material properties, mesh parameters, and miscellaneous input:

Geometric parameters

- trunnion: inner radius, outer radius, and length, and axial position of hub on trunnion.
- hub: inner radius, thickness, width, position of flange, outer radius, flange thickness, location of flange, number of gussets, gusset thickness, and backing ring width.
- girder: web thickness, web height, flange thickness, flange width and length.
- fit: interference between trunnion and hub and hub and girder.

Non-homogeneous material properties

- steel: Young's modulus, Poisson's ratio, thermal conductivity, density, coefficient of thermal expansion specific heat, and fracture toughness versus temperature.
- air: convection heat transfer coefficient versus temperature.
- liquid N_2: convection heat transfer coefficient of liquid nitrogen versus temperature.

Mesh properties

- trunnion: number of elements along trunnion axial length, radius, and circumference.

- hub: number of elements along hub axial length, thickness, radius, and circumference.
- girder: number of elements along flange width and thickness, and web thickness and height, and girder length.

Miscellaneous input

- bridge choice – new or one of four saved bridges.
- assembly procedure #1 or #2.
- thermal (cooling and warming) and structural file names for trunnion, hub, and girder.
- temperature of warming (air) and cooling (liquid nitrogen) mediums.
- time durations and increments for warming in air and cooling in liquid nitrogen for each respective step and component (trunnion, hub or girder) of the process.
- convergence criteria.

FEA Mesh

For a transient thermal-structural analysis of a typical bridge, the mesh consisted of 3,078 8-noded brick elements and 3,756 nodes as shown in Figure 9.

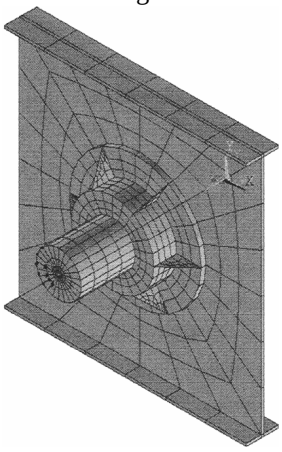

Figure 9. Typical finite element mesh.

The elements used were capable of modeling the coupled thermal (conduction and convection) and structural fields, and the contact and target regions between the trunnion-hub and hub-girder interfaces.

Results

Three bridges (i.e., Christa McAuliffe, Hillsborough Avenue and 17th Street Causeway) were studied using the THGTM. Note that the aim of these finite element studies was to determine which assembly procedure was safer in terms of lower stresses and/or larger allowable crack lengths. First, a comparison of stresses at steady-state at the inner radius of the hub from finite element study (THGTM) [2] with those obtained from the analytical study (BBDT) [1] is presented in Table 5.

Second, a transient thermal-structural analysis was completed for each of the three bridges. A typical contour plot of the hub for AP#2 of Christa McAuliffe Bridge, during the cooling of the hub, is shown in Figure 10. This is the time when the lowest critical crack length is observed.

Table 5. Comparison between THGTM and BBDT results.

Bridge	Stress (ksi)		Percent difference
	THGTM	BBDT	
Christa McAuliffe	9.812	9.372	4.59 %
Hillsborough Ave	10.173	9.813	3.62 %
17th St. Causeway	14.298	13.457	6.06 %

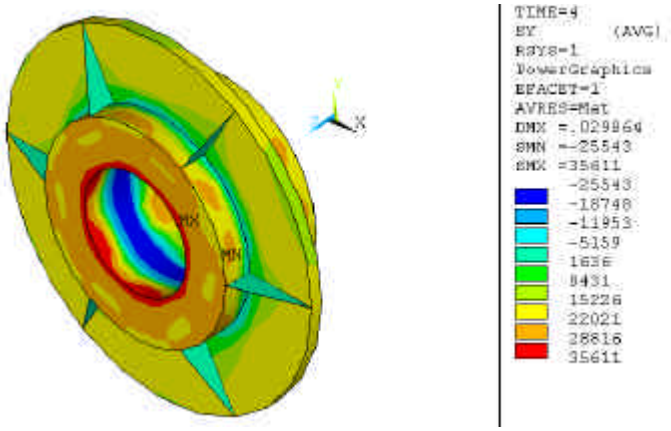

Figure 10. Hoop stress (psi) plot when the highest hoop stress during AP2 is observed (Christa McAuliffe Bridge).

Finally, a comparison of the highest hoop stress and critical crack length, based on the transient thermal-structural analysis, for the three bridges is presented in Table 6. An examination of the results reveals significant differences in the stresses of each THG bridge geometry. In some bridges, a lower critical crack length is found to occur during AP1 (that is, Christa McAuliffe and 17th Street Causeway) while in others (that is, Hillsborough Avenue) the opposite is true, however, only slightly.

Table 6. Critical crack length and maximum hoop stress for different assembly procedures and different bridges.

Bridge	Parameter	Assembly procedure	
		AP#1	AP#2
Christa McAuliffe	Allowable crack length (in)	0.2101	0.2672
	Maximum Hoop Stress (ksi)	28.750	33.424
Hillsborough Avenue	Allowable crack length (in)	0.2651	0.2528
	Maximum Hoop Stress (ksi)	29.129	32.576
17th Street Causeway	Allowable crack length (in)	0.6420	1.0550
	Maximum Hoop stress (ksi)	15.515	17.124

Before looking at the stress results, one needs to note that stresses at a particular point need to be viewed with caution. First, since yield strength of steel increases with a decrease in temperature (Figure 6), allowable stress is dependent on the stresses as well as temperature at that point. Second, since fracture toughness of steel decreases with a decrease in temperature (Figure 6), allowable crack length is dependent on the hoop stress as well as the temperature at that point.

The stresses developed during these two procedures were compared against each other. The hoop stress developed in each bridge is higher for AP#2 versus AP#1, however, this stress occurs at a temperature (not shown in Table 6) when the yield strength is also higher compared to AP#1.

FULL SCALE TESTING

The experimental setup was to measure stresses and temperatures during the two assembly procedures, AP#1 and AP#2. To do so, strain gages and thermocouples were mounted on the trunnion, hub, and girder. These sensors monitored strains and temperatures during all steps of the assembly procedure.

To compare the results from the two assembly procedures, two nearly identical (nominal diameters and interferences at trunnion-hub and hub-girder interfaces were held the same to a tolerance of 1/10,000th of an inch) sets of trunnion, hub and girder were assembled using the two assembly procedures, AP#1 and AP#2. Nominal dimensions of the trunnion, hub, and girder are shown in Table 2. Diametrical interfaces are fixed at 0.0077 in. and 0.0047 in. at the two interfaces.

Strain Gages and Thermocouples

Figure 11 shows details of the positions of the gages on the hub. Each mark in Figure 11 represents a set of one strain gage and one adjacent thermocouple. Based on the location of failure in trunnion-hub assembly of the Christa McAuliffe bridge, the positions of gages of main interest are on the hub inner diameter (Gages-10, 11, 13 and 15).

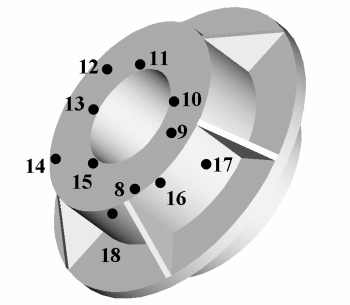

Figure 11. Strain gage and thermocouple locations on the hub.

Experimental Results

Figure 12 presents comparison of the hoop stress on the inner diameter of the hub between AP#1 and AP#2. For AP#1, Step 1 is when the trunnion is immersed in liquid nitrogen. The hoop stress in the hub remains zero during this step. In Step 2, the cold trunnion is inserted into the hub. Consequently, the hoop stress rises to a steady-state value of approximately 12.5 ksi. Step 3 is the most critical step in AP#1 (i.e., trunnion-hub cool down by immersion in liquid nitrogen), resulting in a peak hoop stress of approximately 25.7 ksi. During Step 4 (i.e., trunnion-hub warm-up into the girder), the steady-state stress on the hub inner diameter reaches approximately 12.8 ksi.

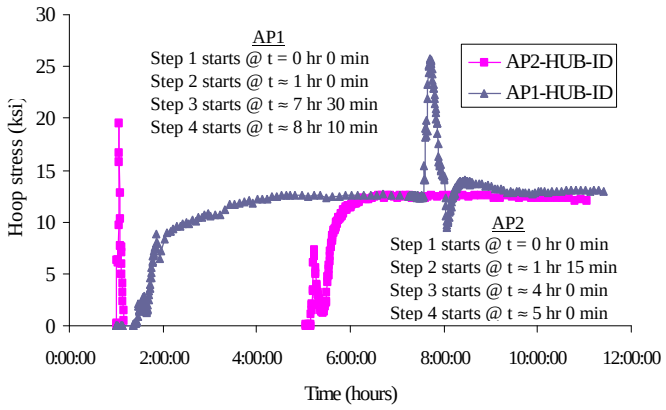

Figure 12. Comparison of the hoop stress during the two assembly procedures, AP#1 and AP#2.

Again, in Figure 12, the plot of hoop stress for AP#2 is also divided into the four assembly steps. Step 1 (hub cool-down by immersion in liquid nitrogen), results in a peak stress of approximately 19.5 ksi on the hub inner diameter. In Step 2, the hub warms up into the girder, and the compressive stress on the hub inner diameter is less than 1 ksi and hence is not noticeable in the graph. Hence, it has been omitted from the plot for the sake of clarity. In Step 3, the trunnion is cooled down by immersion in liquid nitrogen producing no change in stress on the hub. In Step 4, the trunnion expands within the hub, creating tensile stresses on the hub inner diameter. The steady-state value of this stress is approximately 12.1 ksi, which is very close to that of AP#1 (12.8 ksi).

The comparison of AP#1 and AP#2 based on hoop stress should actually be discussed based on the factor of safety (see Table 7) since yield strength of steel varies as a function of temperature (Figure 6). In Table 7, the minimum factor of safety (FOS) is shown and is calculated as the minimum ratio of hoop stress in the hub to the yield strength of steel during the whole assembly procedure.

Figure 13 compares the Von-Mises stresses on the hub inner diameter during the two assembly procedures. The peak stress of 49 ksi in AP#1 is observed in Step 3 (trunnion-hub cool-down by immersion in liquid nitrogen). At this time, the hub has both high radial and hoop stresses that add up to give very high values of Von-Mises stresses. The peak stress of 32 ksi in AP#2 is during Step 4 (warm-up of the trunnion in the hub-girder assembly). It is to be noted that this peak is significantly lower than that of AP#1.

Table 7. Factor of safety (FOS) comparisons of the two assembly procedures (experimental data).

	Assembly procedure	
	AP#1	**AP#2**
Temperature (^{0}F)	-124	-171
Fracture toughness (ksi-$\sqrt{in}$)	32.5	29
Yield strength (ksi)	56	64
Hoop stress (ksi)	19.0	19.5
FOS	2.95	3.29
Time during assembly	4th min. into trunnion-hub cool-down	3rd min. into hub cool-down

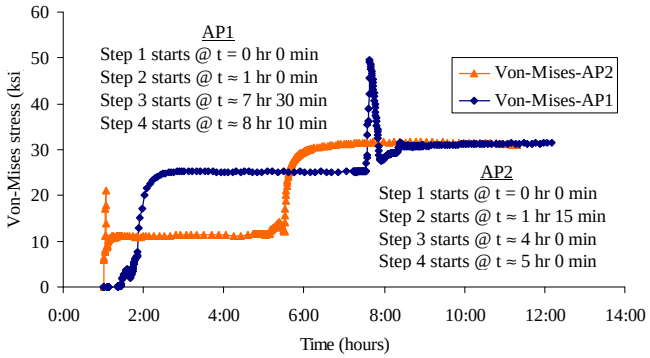

Figure 13. Comparison of Von-Mises stress during the two assembly procedures, AP#1 and AP#2.

Table 8 shows the values of the allowable crack length (ACL) (determined from experimental data) during each of the two assembly procedures. Fracture toughness values are needed to calculate ACL from the hoop stress. It is to be noted from Figure 6 that (a) the fracture toughness decreases with decreasing temperature, and (b) the values of fracture toughness are given for ASTM E-24 steel. Values for actual hub material of sand-cast steel are not available in the literature.

Table 8. Allowable crack length (ACL) comparisons of the two assembly procedures (experimental data).

	Assembly procedure	
	AP#1	**AP#2**
Temperature (^{0}F)	-278	-171
Fracture toughness (ksi-$\sqrt{in}$)	28	29
Yield strength (ksi)	96	65
Maximum hoop stress (ksi)	25.7	19.5
ACL (in)	0.2985	0.5562
Time during assembly	8th min. into trunnion-hub cool-down	3rd min. into hub cool-down

Comparison to FEA Results

Table 9 shows values of ACL as predicted by the finite element analysis (FEA) [2]. The difference between the experimental and the FEA values can be attributed to several reasons, such as, not accounting for taper on the hub and heating of the hub, in the FEA model. We found that the hub had a taper of the same order of magnitude as the interference at the inner diameter. Because of this taper, some aspects of the experimental study had to be altered from the assembly procedure steps mentioned in the introduction. The taper caused the clearance (achieved by the cooling of the trunnion) to be insufficient for a successful assembly. Hence, the hub was heated to 200^{0}F to get an extra 0.01" of clearance.

Table 9. Allowable crack length (ACL) comparisons of the two assembly procedures (FEA data).

	Assembly procedure	
	AP#1	**AP#2**
Temperature (^{0}F)	-92	-92
Fracture toughness (ksi-$\sqrt{in}$)	33.5	33.5
Yield strength(ksi)	53	53
Maximum hoop stress (ksi)	37.0	21.5
ACL (in)	0.2061	0.6106
Time during assembly	3rd min. into trunnion-hub cool-down	1st min. of trunnion warm-up

Summary of Results

Table 10 summarizes the comparisons of assembly procedure 1 (AP#1) and assembly procedure 2 (AP#2) based on all three criteria - hoop stress, Von-Mises stress and ACL. Table 10 clearly illustrates that AP#2 is significantly better compared to AP#1 in terms of all three criteria, although, these results may or may not significantly change by changing the geometry or interference values in the THG assembly. The FEA results (see Table 9) are in agreement with this conclusion as well.

Table 10. Comparisons of AP#1 and AP#2 summary.

	Assembly Procedure	
	AP#1	**AP#2**
Maximum hoop stress (ksi)	25.7	19.5
Maximum Von-Mises Stress (ksi)	49.2	30.9
FOS	2.95	3.29
ACL (in)	0.2985	0.5562

Since yield strength increases with a decrease in temperature, maximum hoop stresses do not necessarily result in lower values of factors of safety. Also, note that the maximum Von-Mises stress does not coincide with the time when the maximum hoop stress occurs in AP#2. The maximum Von-Mises stress occurs when the whole assembly reaches steady-state. Whereas, the maximum hoop stress occurs due to thermal shock when the hub is cooled down by immersion in liquid nitrogen.

The numbers for ACL in Table 10 were calculated at all the locations of the strain gages at different times and the smallest number gives the allowable crack length for the whole

assembly. Note that as the temperature decreases, the fracture toughness decreases (see Figure 6), and hence, the value of the ACL decreases.

RECOMMENDATIONS

Based on the results of this study, the following recommendations were made for the THG assembly procedure:

1. Develop inspection specifications for determining if voids or cracks in the cast hub are bigger than an allowable value. This value would vary depending on the THG geometry, interference values, materials used, cooling method, etc.
2. Specify tight machining tolerances for the inner diameter of the hub, indicating true position and perpendicularity tolerances. A taper along the depth could contribute to chances of the trunnion getting stuck in the hub during assembly procedure (for example, during THG assembly of Venetian Causeway) or possibly create larger interference stresses than necessary.
3. Consider heating the outer component as an alternative to cooling the inner component as heating is a slow process and hence does not create large transient thermal stresses, and heating the steel does not lower the fracture toughness appreciably as cooling.
4. Consider gradual cooling of the hub being cooled by itself (AP#2) or as a trunnion-hub assembly (AP#1) in a convection-cooling chamber using liquid nitrogen as opposed to immersion in liquid nitrogen. This will avoid thermal shock associated with direct immersion. The drawback is that it would be slower to carry out.
5. Consider staged cooling wherein the trunnion or hub is first cooled from room temperature to 0^0F in a refrigerator, and then cooled in dry-ice/alcohol to -109^0F, before being cooled to -321^0F in liquid nitrogen. This staged cooling is better than immersing directly in liquid nitrogen since in any given stage the temperature change is smaller, resulting in significantly lower transient stresses.

The FDOT has implemented the recommendations of this research, the major one being the heating of the outer component of the assembly (called AP#3 henceforth). Instead of cooling the trunnion-hub assembly in AP#1, the girder could be warmed using induction coils. Cooling in liquid nitrogen gives a temperature change of –401^{o}F assuming an ambient temperature of 80^{o}F. Because the coefficient of thermal expansion of steel decreases with temperature (Figure 7), an equivalent thermal strain could be attained if the girder was heated through a temperature change of approximately 280^{o}F. This means that enough clearance would result by heating the girder to approximately 360^{o}F, which is far below any temperature that would change the mechanical properties of the material. In other words, heating the girder to 360^{o}F (below a temperature that would change the material's mechanical properties) yields the same clearance for assembly as cooling the trunnion-hub to –321^{o}F. The heating of the outer component has a significant effect on the assembly process in that relatively higher clearances are obtained with reduced thermal gradients and stresses, as compared to the cooling of the inner component.

ACKNOWLEDGEMENTS

This work was supported by the FDOT through contract number B-C008 to USF, Tampa. We acknowledge the expertise provided by Mr. Jack Evans and Mr. Angel Rodriguez of the FDOT. We wish to thank Mr. James Allison, PE of Steward Machine Co. in Birmingham, AL for machining the trunnion, hub, and girder test specimens. We are grateful to Mr. Paul Hillis of PGH Engineering in Tampa, FL for his pragmatic insight into the assembly of a trunnion-hub-girder. Thanks to Mr. George Patton of EC Driver in Tampa, FL for his assistance during the project.

REFERENCES

[1] Denninger, M. T., 2000, "Design Tools for Trunnion-Hub Assemblies for Bascule Bridges." MS Thesis, Mech. Eng. Dept., Univ. of S. Florida, FL.

[2] Ratnam, B., 2000, "Parametric Finite Element Modeling of Trunnion Hub Girder Assemblies for Bascule Bridges." MS Thesis, Mech. Eng. Dept., Univ. of S. Florida, FL.

[3] Nichani, S., 2001, "Full Scale Testing of Trunnion-Hub-Girder Assembly of a Bascule Bridge." MS Thesis, Mech. Eng. Dept., Univ. of S. Florida, FL.

[4] Besterfield, G.H., Kaw, A.K., and Crane, R.A., 2001, "Parametric Finite Element Modeling and Full-Scale Testing of Trunnion-Hub-Girder Assemblies for Bascule Bridges", Florida Department of Transportation Contract Report – Contract #B-C008, Mech. Eng. Dept., Univ. of S. Florida, FL.

[5] "Bascule Bridge Trunnion-Hub-Girder Designer", 2001, <http://www.eng.usf.edu/~besterfi/bascule> (April 15, 2002).

[6] Shigley, J.E. and Mischke, C. R., 1986, Chapter 19 - Limits and Fits, *Standard Handbook of Machine Design*, McGraw-Hill, New York.

[7] Ugural, A. C. and Fenster, S. K., 1995, *Advanced Strength and Applied Elasticity*, Third Edition, Prentice Hall, New York.

[8] Kanninen, M. F. and Popelar, C. H., 1985, *Advanced Fracture Mechanics, Oxford Engineering Science Series*, Oxford University Press, New York.

[9] Greenberg, H. D., and Clark, Jr. H.G., 1969, "A Fracture Mechanics Approach to the Development of Realistic Acceptance Standards for Heavy Walled Steel Castings", Metals Engineering Quarterly, 9(3), 30-33.

[10] Brentari E. G. and Smith R. V., 1964, "Nucleate and Film Pool Boiling Design Considerations for 0_2, N_2, H_2 and He," *International Advances in Cryogenic Engineering*, 10b, pp. 325-341.